J Herbmed Pharmacol. 2026; 15(1): 66-74.

http://www.herbmedpharmacol.com doi: 10.34172/jhp.2026.53250

Journal of Herbmed Pharmacology

Phytochemical characterization and biological evaluation of *Carica papaya* L. leaf alkaloids: *In vitro* and *in silico* insights into antioxidant, cytotoxicity, and anti-inflammatory activities

Arya J[1,2], Krishnakumar K[1], Alex George[3], Remya Chandran[4], Akash Prakash[2], Mathew John[2*]

[1]Nutraceuticals Research Division, Department of Botany, Maharaja's College (Government Autonomous), Ernakulam, 682011, Affiliated to Mahatma Gandhi University,Kerala, India
[2]Biochemistry and Phytochemistry Research Division, Jubilee Centre for Medical Research, Jubilee Mission Medical College and Research Institute, Thrissur, 680005, Kerala, India
[3]Cell and Molecular Biology Facility, Jubilee Centre for Medical Research, Jubilee Mission Medical College and Research Institute, Thrissur, 680005, Kerala, India
[4] Laboratory for Computational and Structural Biology, Jubilee Centre for Medical Research, Jubilee Mission Medical College and Research Institute, Thrissur, 680005, Kerala, India

ARTICLE INFO

Article Type:
Original Article

Article History:
Received: 5 Jul. 2025
Revised: 3 Nov. 2025
Accepted: 3 Nov. 2025
epublished: 1 Jan. 2026

Keywords:
Carpaine
Carpamic acid
Cyclooxygenase-2
Nitric oxide
Cytotoxicity

ABSTRACT

Introduction: *Carica papaya* L. leaf alkaloids have gained pharmacological interest for their anti-thrombocytopenic activity. Inflammation and oxidative stress exacerbate disease severity. This study evaluated the *in vitro* antioxidant, cytotoxicity, and anti-inflammatory activities of the alkaloid fraction of *C. papaya* leaves.
Methods: The alkaloid fraction was isolated and analyzed using ultra-performance liquid chromatography-quadrupole time-of-flight mass spectrometry (UPLC-QTOF-MS/MS) and Fourier transform infrared (FTIR) spectroscopy. Antioxidant potential was evaluated by the 2,2-diphenyl-1-picrylhydrazyl (DPPH) and ferric-reducing antioxidant power (FRAP) assays. Cytotoxicity was determined by the 3-(4,5-dimethylthiazol-2-yl)-2,5-diphenyltetrazolium bromide (MTT) assay. Anti-inflammatory potential was assessed by quantifying cyclooxygenase-2 (COX-2), inducible nitric oxide synthase (iNOS) activities, and cellular nitrite levels in LPS-stimulated RAW 264.7 macrophage cells. *In silico* analysis was performed to assess the binding interactions of alkaloid compounds with COX-2 and iNOS.
Results: Carpaine and carpamic acid were identified as potential alkaloid compounds. DPPH assay demonstrated concentration-dependent antioxidant activity (IC_{50} = 0.77 (0.06) mg/mL), and FRAP assay showed potential ferric-ion-reducing ability. COX-2 and iNOS activities were significantly decreased ($P < 0.01$) with IC_{50} values of 31.02 (4.53) µg/mL and 28.85 (3.27) µg/mL, respectively**.** Nitric oxide production decreased in a concentration-dependent manner ($P < 0.01$). *In silico* analysis revealed that carpamic acid had a stronger binding affinity for iNOS and COX-2 compared to carpaine. MTT assay demonstrated cytotoxicity with an LC_{50} of 49.69 (0.89) µg/mL and a favorable selectivity index.
Conclusion: The alkaloid fraction of *C. papaya* leaves exhibits significant antioxidant, cytotoxicity, and anti-inflammatory activities at non-toxic concentrations. Further *in vivo* studies are needed to validate and expand on the current findings.

Implication for health policy/practice/research/medical education:
The alkaloid fraction of *Carica papaya* L. leaves demonstrated significant antioxidant, cytotoxicity, and anti-inflammatory properties at non-toxic concentrations, highlighting its potential phytopharmaceutical application in managing these pathophysiological conditions.

Please cite this paper as: J A, K K, George A, Prakash A, John M. Phytochemical characterization and biological evaluation of *Carica papaya* L. leaf alkaloids: *In vitro* and *in silico* insights into antioxidant, cytotoxicity, and anti-inflammatory activities. J Herbmed Pharmacol. 2026;15(1):66-74. doi: 10.34172/jhp.2026.53250.

***Corresponding author**: Mathew John,
Email: mathewjohn@jmmc.ac.in

Introduction

Carica papaya L. is widely cultivated in subtropical and tropical countries for its fruit (1). Traditionally, its leaf preparations have been used against ulcers, hypertension, diabetes, bacterial infections, dengue, malaria, and constipation (2). Among its diverse therapeutic potentials, several studies have highlighted the role of crude *C. papaya* leaf extracts in addressing thrombocytopenia by enhancing platelet production and modulating immune responses (3-5).

Carica papaya leaves are rich in pharmacologically important secondary metabolites, including phenols, glycosides, steroids, flavonoids, saponins, tannins, and alkaloids. Alkaloids in papaya leaves have demonstrated significant bioactivities (2). They have been previously studied for their cardioprotective and spasmolytic effects (6). In another study, *C. papaya* alkaloids demonstrated a significant *in vitro* anti-plasmodial activity (7). They have also been shown to promote the proliferation of H9c2 cardiomyocytes through FAK-ERK1/2 and FAK-AKT signalling pathways (8). Alkaloids from *C. papaya* leaves have recently gained significant therapeutic interest for their anti-thrombocytopenic property (9). However, their potential in mitigating oxidative stress and inflammation has not been much explored. Oxidative stress and inflammation are involved in the progression and severity of pathophysiological conditions, such as thrombocytopenia. Inflammatory responses exacerbate thrombocytopenic conditions by causing endothelial dysfunction and increasing vascular permeability, thereby triggering bleeding (10). One of the common causes of thrombocytopenia is dengue virus infection (11). In severe dengue infection, a cytokine storm contributes to disease severity by intensifying inflammatory and oxidative stress responses (12). An altered cytokine profile in dengue patients impairs the stromal cells and bone marrow function, leading to thrombocytopenia (13). Inflammation also leads to increased peripheral platelet destruction (14). Therefore, mitigating free radical production and inflammation is crucial for managing thrombocytopenic conditions and preventing associated complications. This study aimed to isolate and characterize the alkaloid fraction from *C. papaya* leaf and evaluate its *in vitro* antioxidant and anti-inflammatory potential.

Materials and Methods

Cell lines, chemicals, and reagents

RAW 264.7 macrophage cells were procured from the National Centre for Cell Sciences, Pune, India. DPPH, lipopolysaccharide (LPS), dimethyl sulfoxide (DMSO), MTT, calcium chloride, ascorbic acid, trichloroacetic acid, and Dulbecco's modified Eagle's medium (DMEM) were purchased from Sigma Aldrich, USA. All other analytical grade solvents and chemicals were purchased from Merck, Germany.

Plant material and preparation of alkaloid fraction

Mature leaves of *Carica papaya* L. were collected from the Jubilee Mission Medical College Garden, Thrissur, Kerala, and authenticated (voucher specimen no: 123770; Calicut University herbarium). *C. papaya* leaf alkaloid fraction (CPL-AL) was isolated as previously described (15). Alkaloids were detected using Dragendorff's reagent.

Ultra-performance liquid chromatography-quadrupole time-of-flight mass spectrometry

Chemical composition of CPL-AL was analyzed using UPLC-Q-TOF-MS/MS analysis. Chromatographic separation was conducted using an Acquity UPLC BEH C18 column (50 mm × 2.1 mm × 1.7 µm) from Waters connected to an Xevo G2QTOF mass spectrometer with an electrospray ionization source. The mobile phase consisted of 0.1% formic acid in water (mobile phase A) and acetonitrile (mobile phase B), with a gradient of 95:5 at 0 minutes, 5:95 at 6 minutes, and then 95:5 at 9 minutes (flow rate, 300 µL/min). The m/z scan range was from 50 to 1000. The collision energy range was 5-30 eV. Gas flow (nitrogen) was at a rate of 900 L/h at a temperature of 350 °C. MassLynx software (v4.1) was used for data acquisition and analysis (16). The compounds were further identified using the ChemSpider and PubChem databases, and their elemental composition and accurate mass were compared with previously reported values.

Fourier transform infrared spectroscopy (FTIR)

FTIR analysis of CPL-AL was performed using a Thermo Nicolet iS50 FTIR spectrometer (Thermo Fisher Scientific, USA) in the spectral range of 4000–100 cm^{-1}, and a spectral resolution of 0.2 cm^{-1}. CPL-AL was coated on a KBr pellet for the analysis. The peak values were used to identify functional groups.

Antioxidant assays

2,2-Diphenyl-1-picrylhydrazyl (DPPH) assay

DPPH (100 µL of 500 µM) was mixed with 100 µL of CPL-AL (0.1 mg/mL to 1.6 mg/mL) and incubated in the dark at room temperature for 30 minutes. DPPH without CPL-AL served as the negative control. Ascorbic acid (0.2 mg/mL) was used as the reference standard. Absorbance was measured at 517 nm using a Tecan Infinite 200 Pro multimode plate reader (16). The percentage DPPH inhibition was calculated as:

$$DPPH\ inhibition\% = \frac{(Absorbance\ of\ control - Absorbance\ of\ sample)}{Absorbance\ of\ control} \times 100$$

Ferric-reducing antioxidant power (FRAP) assay

The FRAP assay was used to assess the reducing potential of CPL-AL (16). 100 µL of CPL-AL (0.1 to 1.6 mg/mL) was incubated with 100 µL of 1% potassium ferricyanide for 20 minutes at room temperature. Subsequently, 70 µL

of 0.1% ferric chloride was added, and the mixture was incubated for 5 minutes. The absorbance of the samples was measured at 700 nm using a multimode reader. The results were expressed as ascorbic acid equivalent (AAE) in μg/mL.

Cytotoxicity assay

The RAW 264.7 macrophage cells were suspended in 10% growth medium and seeded in tissue culture plates at a density of 5×10^3 cells per well, followed by 24 hours of incubation. Cells were then incubated with different concentrations of CPL-AL dissolved in DMEM (6.25-100 μg/mL), each in triplicate, and incubated for an additional 24 hours. After treatment, 5 mg/mL (10 μL) MTT solution was added and incubated at 37 °C (4 hours). Following incubation, the formazan crystals formed were solubilized in DMSO (100 μL). Untreated cells served as the negative control. The absorbance was measured at 570 nm in a microplate reader (17). The cell viability was calculated as:

$$Cell\ viability\% = \frac{Absorbance\ of\ sample}{Absorbance\ of\ control} \times 100$$

Anti-inflammatory assays

For anti-inflammatory assays, 5×10^3 cells/well were activated with 1 μg/mL LPS (1 μL), followed by treatment with non-toxic concentrations of CPL-AL for 24 hours, except in the negative control. The cell lysates were collected for subsequent anti-inflammatory assays (18). Diclofenac was used as the reference standard.

Cyclooxygenase-2 activity

The cyclooxygenase-2 (COX-2) inhibition was determined as described previously, with minor modifications (19). 5mM hemoglobin, Tris-HCl buffer (pH 8), and 5mM glutathione were added to the cell lysate (100 μL) and incubated at 25 °C for 1 minute. 200 mM arachidonic acid was added to initiate the reaction, followed by 20 minutes of incubation at 37 °C. 10% trichloroacetic acid (200 μL) was added to terminate the reaction. After centrifugation, 1% thio-barbituric acid (200 μL) was added, and the tubes were boiled for 20 minutes, cooled, and centrifuged for 3 minutes at 1000 rpm. COX-2 activity was evaluated by measuring absorbance at 632 nm and calculated as:

$$\text{COX-2 inhibition\%} = \frac{(\text{Absorbance of control-Absorbance of sample})}{\text{Absorbance of control}} \times 100$$

Inducible nitric oxide synthase activity

The cell lysate was homogenized in 100 mM (2 mL) HEPES buffer (pH 7.5). The reaction mixture (0.1 mL each) consists of 2 μM L-arginine, 1mM NADPH, 4 μM manganese chloride, 10mM dithiothreitol (DTT), 4 μmM tetrahydropterin, 10 μM oxygenated hemoglobin, and cell lysate. After incubating for 15 minutes, the absorbance was measured at 401 nm (20). The percentage of iNOS inhibition was determined as:

$$\text{iNOS inhibition\%} = \frac{(\text{Absorbance of control-Absorbance of sample})}{\text{Absorbance of control}} \times 100$$

Estimation of cellular nitrite levels

Cellular nitrite levels were determined according to Lepoivre et al, with minor modifications (21). Cell lysate (0.5 mL) was mixed with 3% sulfosalicylic acid (0.1 mL), vortexed for 30 minutes, and then centrifuged at 5000 rpm for 15 minutes. The protein-free supernatant (200 μL) was mixed with 10% NaOH (30 μL) and Tris-HCl buffer (300 μL), followed by the addition of 530 μL of Griess reagent. The mixture was incubated in the dark for 15 minutes. The absorbance was measured at 540 nm. Sodium nitrite was used as the standard, and the nitrite levels were estimated from the standard curve. Griess reagent served as the blank.

The selectivity index (SI) of CPL-AL for COX-2 and iNOS inhibition was calculated by dividing the cytotoxicity by the anti-inflammatory effectiveness to ascertain the efficacy of CPL-AL (22).

In silico analysis

Molecular docking was performed to elucidate the inhibitory mechanism of compounds in CPL-AL against COX-2 and iNOS. The crystal structure of human COX-2 (PDB ID: 5IKQ) and human iNOS heme domain (PDB ID: 4CX7) were selected for docking. Each protein was prepared using the Protein Preparation Wizard by adding hydrogen and other missing atoms and removing water molecules. The hydrogen bond network was optimized, and restrained energy minimization was performed using the OPLS3 force field. Prepared ligands were docked using the extra precision (XP) docking protocol in the Schrödinger Maestro program. The free energies of binding of the docked complexes were subsequently calculated using Prime MM-GBSA.

Molecular dynamics simulation (MDS) was performed using the GPU-enabled Desmond program to assess the stability and dynamic behavior of the ligands within the active sites of COX-2 and iNOS. Prior to simulations, each protein–ligand complex was prepared with the System Builder tool in Desmond. The complexes were placed in an orthorhombic box of 9 × 9 × 9 Å and solvated using the TIP3P explicit water model. Sodium or chloride ions were also added as counter-ions to neutralize the system. The simulations were carried out for 250 ns using the OPLS-2005 force field, with trajectories recorded every 250 ps. All simulations were performed under an NPT ensemble at 300 K and 1.01 (23,24).

Data analysis

All in vitro experiments were performed in triplicate. The data were presented as median with interquartile range

(IQR). Lethal concentration 50 (LC_{50}) and inhibitory concentration at 50% (IC_{50}) were determined using ED50 PLUS V1.0 software. The analysis was performed using GraphPad Prism version 10.5.0 (774), and statistical significance was determined by the Kruskal–Wallis test followed by Dunn's post-hoc multiple comparisons test. $P < 0.05$ was considered statistically significant.

Results

Yield and phytochemical composition

The percentage yield of CPL-AL was 0.78% w/w. It was obtained as a sticky, dark yellow solid mass. UPLC-Q-TOF-MS/MS analysis revealed the presence of 7 nitrogen-containing compounds, among which carpaine, carpamic acid, methyl carpamate, and 6-(8-methoxy-8-oxooctyl)-2-methylpiperidine-3-yl8-(5-hydroxy-6-methylpiperidine-2-yl) octanoate were identified. Carpaine and carpamic acid were identified by MassLynx software. Methyl carpamate and 6-(8-methoxy-8-oxooctyl)-2-methylpiperidine-3-yl 8-(5-hydroxy-6 methylpiperidine-2-yl) octanoate were identified using previous literature (7). All compounds were detected in the positive ionization mode (Table 1).

FTIR spectral analysis

FTIR spectrum of CPL-AL showed 9 prominent peaks. The functional groups identified included O-H, C-H, C=O, N-H, C-N, and C-O (Table 2).

Antioxidant activity

The antioxidant activity of CPL-AL was estimated using the DPPH assay. The percentage of DPPH scavenging was found to be concentration-dependent (Figure 1A). CPL-AL showed significant DPPH inhibition compared to the negative control ($P < 0.01$), with an IC_{50} value of 0.77 (0.06) mg/mL. The reference standard ascorbic acid showed 96% activity at a concentration of 0.2 mg/mL.

The FRAP assay evaluated the ability of compounds to reduce a Fe^{3+} complex in the FRAP reagent to Fe^{2+}. An increase in absorbance indicated an increased reduction of ferrous ions. The reducing ability of CPL-AL was found to be concentration-dependent (Figure 1B).

Table 2. Fourier transform infrared (FTIR) analysis of *Carica papaya* L. leaf alkaloid fraction

Wave numbers (cm^{-1})	Functional groups	Compound class
3322.70	O-H	Carboxylic acid
2923.82	C-H stretch	Alkane
2853.51	C-H stretch	Alkane
1727.03	C=O stretch	Ester
1590.85	N-H bend	Amine
1443.22	O-H bend	Carboxylic acid
1376.02	O-H bend	Alcohol
1247.47	C-N stretch	Amine
1050.67	C-O stretch	Ester

Cytotoxicity analysis

Cytotoxicity of CPL-AL was determined by MTT assay on the RAW 264.7 macrophage cell line. The cell viability decreased in a concentration-dependent manner over the range of 6.25-100 µg/mL (Figure 2A). LC_{50} was found to be 49.69 (0.89) µg/mL. Concentrations maintaining above 80% cell viability (3.12, 6.25, and 12.5 µg/mL) were selected for assessing the anti-inflammatory potential.

Anti-inflammatory activity

The anti-inflammatory activity of CPL-AL was evaluated by examining its influence on COX-2 activity, iNOS expression, and cellular nitrite production in LPS-stimulated RAW 264.7 macrophage cell line. CPL-AL reduced COX-2 activity compared to the negative control with a significant difference at the highest chosen concentration ($P < 0.01$) (Figure 2B). The IC_{50} value of CPL-AL was 31.02 (4.53) µg/mL, which was comparable ($P > 0.05$) to that of NSAID (non-steroidal anti-inflammatory drug) diclofenac (IC_{50} value of 23.54 (1.04) µg/mL).

Similarly, CPL-AL exhibited a marked concentration-dependent suppression of iNOS expression (Figure 2C),

Table 1. Phytochemical composition of *Carica papaya* L. leaf alkaloid fraction

RT (min)	m/z	Molecular formula	Proposed compound	Main fragments
2.88	258	$C_{14}H_{27}N_{O}3$	Carpamic acid	258, 240, 222, 109
3.108	479	$C_{28}H_{50}N_{2O}4$	Carpaine	461, 240, 222, 98
3.188	272	$C_{15}H_{29}N_{O}3$	Methyl carpamate	254, 240, 222, 95, 70
3.43	511	$C_{29}H_{54}N_{2O}5$	6-(8-Methoxy-8 oxooctyl)-2-methylpiperidine-3-yl8-(5 hydroxy-6 methylpiperidine-2-yl) octanoate	258, 254, 186, 70
3.673	495	$C_{28}H_{50}N_2O_5$	Unidentified	477, 391, 279, 222
3.796	565	$C_{35}H_{52}N_{2O}4$	Unidentified	344, 326, 240, 129
4.13	358	$C_{22}H_{31}NO_3$	Unidentified	340, 326, 306, 248, 183, 129

Analysis was performed by ultra-performance liquid chromatography-quadrupole time-of-flight mass spectrometry (UPLC-Q-TOF-MS/MS). RT: retention time in minutes; m/z: mass/charge ratio. All compounds were detected in the positive ionization mode.

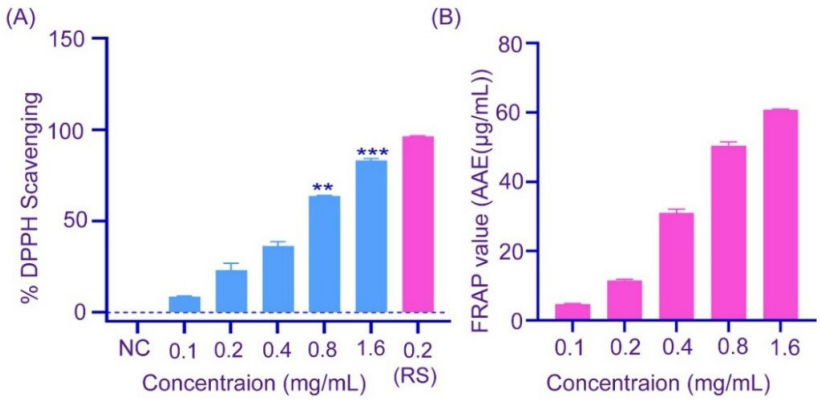

Figure 1. Antioxidant activity of *Carica papaya* L. leaf alkaloid fraction. (A): 2, 2-diphenyl-1-picrylhydrazyl (DPPH) assay. (B): Ferric reducing antioxidant power (FRAP) assay expressed as FRAP value (ascorbic acid equivalent (AAE)). $^{**}P < 0.01$ and $^{***}P < 0.001$ compared to negative control (NC, DPPH+methanol). 0.2 mg/mL ascorbic acid served as the reference standard (RS). The assays were performed in triplicate; data are presented as median with interquartile range.

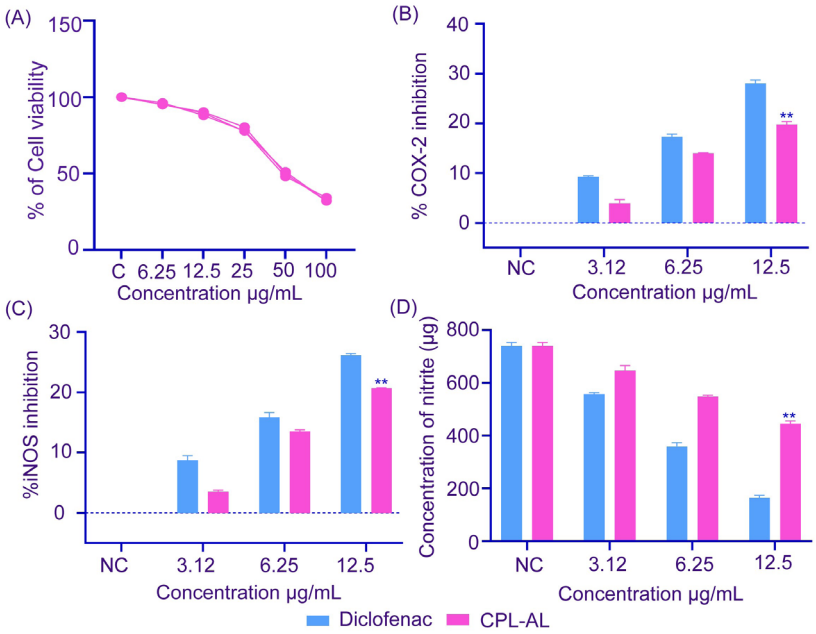

Figure 2. Effect of *Carica papaya* L. leaf alkaloid fraction (CPL-AL) on cell viability and pro-inflammatory mediators. (A) The 3-(4,5-dimethylthiazol-2-yl)-2,5-diphenyltetrazolium bromide (MTT) assay was used to evaluate cell viability. Anti-inflammatory effects of CPL-AL and diclofenac were assessed on (B) cyclooxygenase-2 (COX-2), (C) inducible nitric oxide synthase (iNOS), and (D) cellular nitrite. The assays were performed in triplicate; data are presented as median with interquartile range. $^{**}P < 0.01$ compared to negative control (NC, lipopolysaccharide (LPS) alone). No significant difference was observed between diclofenac and CPL-AL.

showing a significant difference at the highest chosen concentration ($P<0.01$) and an IC50 value of 28.85 (3.27) μg/mL. Cellular nitrite production was also significantly reduced in a concentration-dependent manner (Figure 2D). The nitrite concentration in the culture supernatant at the highest treatment concentration showed a median (IQR) value of 446 (13.4) μg/mL, compared to 740.5 (22.3) μg/mL in the negative control, indicating a significant reduction ($P<0.01$). CPL-AL and the standard drug diclofenac exhibited comparable inhibition of iNOS and cellular nitrite, with no significant difference between the two treatments (Figure 2D).

The selectivity indices for COX-2 and iNOS inhibition were 1.60 and 1.72, respectively. The higher selectivity index (SI>1) indicates selective anti-inflammatory activity over cellular toxicity.

In silico analysis

Carpaine and carpamic acid (Figure 3A and 3B) were chosen as ligands against COX-2 and iNOS enzymes.

Molecular docking studies revealed the distinct atomic-level interactions of the identified alkaloids. In the case of COX-2, carpamic acid successfully occupied the active site (Figure 3C). Its carboxyl group formed stable hydrogen bonds with Arg120 and Tyr355 at the catalytic pocket, with a free energy of binding of –54 kcal/mol, indicating strong affinity. The piperidine moiety of carpamic acid was oriented within a hydrophobic core, engaging in additional interactions with Tyr385 and Met522. MDS revealed that these hydrogen bonds persisted for more than 90% of the trajectory, reflecting the stability of carpamic acid within the COX-2 active site with a low root mean square deviation (RMSD) value (average RMSD = 2.07 ± 0.22 Å) (Figure 3D and 3E). In contrast, carpaine failed to fit within the catalytic pocket.

In the case of iNOS, both carpaine and carpamic acid were successfully accommodated within the enzyme's binding site (Figure 4A and 4B). The binding energies

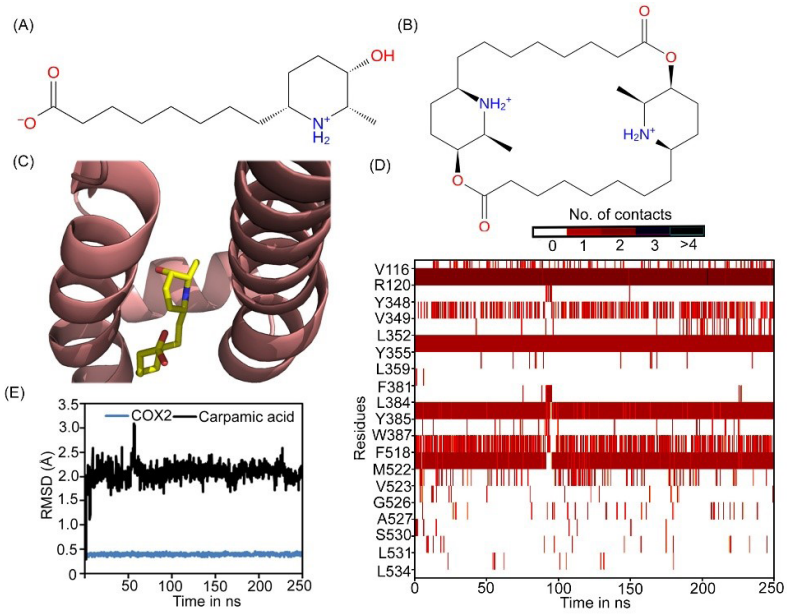

Figure 3. Binding mode of carpamic acid with cyclooxygenase-2 (COX-2). (A) and (B): The chemical structures of carpamic acid and carpaine, respectively. (C) The binding mode of carpamic acid within the COX-2 active site is depicted, with the ligand represented as yellow sticks and the protein as a salmon-coloured cartoon. (D) The interaction profile of key residues with carpamic acid. Darker shades indicate residues forming multiple specific contacts with the ligand. (E) Root Mean Square Deviation (RMSD) profile of carpamic acid.

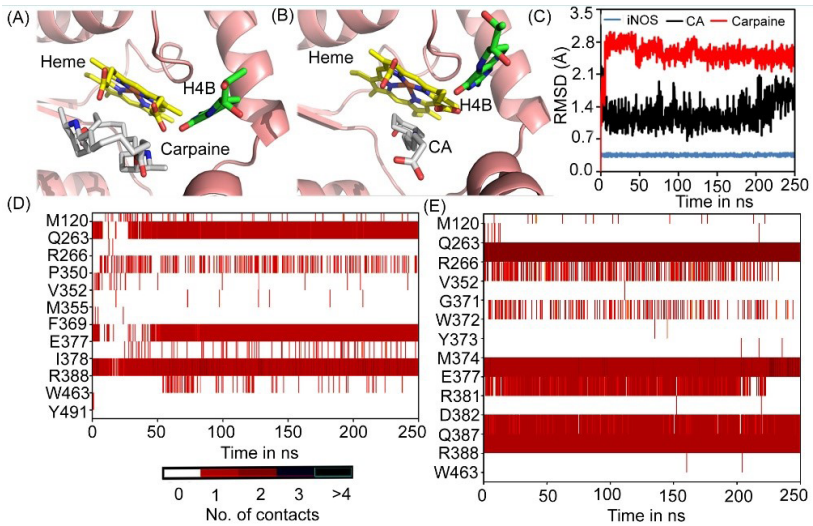

Figure 4. Binding modes of alkaloids with inducible nitric oxide synthase (iNOS). (A) and (B) show binding modes of carpaine and carpamic acid (CA), respectively, within the iNOS active site. The protein is depicted as a salmon-coloured cartoon, while the ligands are represented by white sticks. The heme prosthetic group and the tetrahydrobiopterin cofactor are represented as yellow and green sticks, respectively. (C) represents the root mean square deviation (RMSD) profiles of both alkaloids within the iNOS active site. Specific residue–ligand contact maps for carpaine (D) and carpamic acid (E), where darker shades denote residues exhibiting multiple persistent interactions.

of carpaine and carpamic acid were –60.40 and –64.21 kcal/mol, respectively. Carpaine established hydrogen bonds with Gln263, Glu377, and Arg388. The ligand also made contact with the heme moiety through one of its piperidine nitrogen atoms. Carpamic acid formed highly persistent hydrogen bonds with Glu377, Arg388, and Arg266, indicating a well-stabilized interaction network. MDS revealed that carpaine underwent an initial conformational adjustment before stabilizing (RMSD ~2.5 Å) (Figure 4C), with key interactions persisting for over 80% of the simulation time (Figure 4D). Carpamic acid exhibited stronger and more stable binding within the iNOS active site (RMSD of ~1.25 Å) with key interactions persisting for over 72% of the simulation time (Figure 4C and 4E).

Discussion

The significance of exploring the antioxidant and anti-inflammatory properties of CPL-AL extends to its health-related applications, particularly during disease conditions like dengue fever (25). One of the key contributors to dengue disease pathogenesis is reactive oxygen species (ROS), which accumulate within infected cells shortly after virus entry. In severe conditions, oxidative stress is accompanied by the release of elevated amounts of proinflammatory cytokines in the blood, exacerbating the inflammatory response (26,27).

Dietary intake of natural small-molecule antioxidants is reported to have health benefits against oxidative stress-induced disorders (28,29). The antioxidant properties of papaya leaves have been attributed to their phenolics and flavonoids, which are correlated with their aromatic nature and the presence of hydroxyl groups (16,30,31). However, the antioxidant properties of *C. papaya* leaf alkaloids remain underexplored as per the existing literature. In the present investigation, CPL-AL exhibited significant DPPH scavenging activity, although its IC_{50} value was higher than that of the flavonoid fraction from papaya leaves (16). FRAP assay demonstrated a concentration-dependent increase in absorbance, indicating the metal-reducing potential of CPL-AL. This further ascertains the antioxidant property of CPL-AL.

The major structural motif of potential antioxidant molecules includes the presence of hydroxyl groups, carboxylic acid groups, amino groups, isoprenoid groups, and thiol groups (28,32). In our study, compounds associated with the observed bioactivity were analysed using UPLC-QTOF-MS/MS. Among the identified compounds, carpaine and carpamic acid have been reported for their natural occurrence. Carpaine belongs to the piperidine class of alkaloids, characterized by two identical piperidine rings linked together by two ester groups (6). In contrast, methyl carpamate and 6-(8-Methoxy-8-oxooctyl)-2-methylpiperidine-3-yl8-(5-hydroxy-6-methylpiperidin-2-yl) octanoate are reported as degradation products of carpamic acid or carpaine and are structurally closely related to carpaine (7). FTIR spectral analysis identified the functional groups of compounds in CPL-AL. The observed O-H stretching and bending vibrations could be attributed to the carboxylic acid moiety of carpamic acid, while C=O can be attributed to the lactone structure of carpaine. N-H, C-H, C-O and C-N vibrations can be attributed to both carpaine and carpamic acid (33). As carpaine lacks a hydroxyl group in its structure, the plausible explanation for the observed antioxidant activity could be due to the secondary amino (-NH) group of carpaine and the carboxylic acid (-COOH) group of carpamic acid.

The anti-inflammatory potential of CPL-AL was assessed using multiple parameters. Compounds that are capable of modulating various pro-inflammatory mediators in activated macrophages are of considerable pharmaceutical applications (34). In the present study, CPL-AL treatment exhibited concentration-dependent downregulation of key mediators of inflammation, including COX-2, iNOS, and cellular nitric oxide. CPL-AL significantly inhibited COX-2 activity in LPS-stimulated macrophages with an IC_{50} comparable to that of the standard drug diclofenac (P >0.05), making it a potential candidate for COX-2 inhibition.

Overproduction of cellular nitrite leads to tissue damage and oxidative stress, which in turn fuels chronic inflammation (34). Notably, during conditions such as dengue virus infection, elevated proinflammatory responses, including iNOS and nitrite production, can lead to endothelial cell damage and vascular leakage, which can be fatal (35,36). CPL-AL significantly decreased iNOS activity and nitrite production in a concentration-dependent manner, supporting its anti-inflammatory potential.

Molecular docking and MDS revealed that carpamic acid formed more stable hydrogen bonds with COX-2 and iNOS. Carpaine could not occupy the active site of COX-2, likely due to its macrocyclic structure, which introduced significant steric hindrance and reduced its compatibility with the COX-2 binding cavity (37). The lower IC_{50} value of CPL-AL towards iNOS may be attributed to the interaction of both the alkaloid compounds within the iNOS active site, leading to the suppression of downstream pro-inflammatory mediators.

MTT assay showed that the cytotoxicity of CPL-AL had an LC_{50} of 49.69 µg/mL. The selectivity index of CPL-AL for COX-2 and iNOS inhibition falls under the favorable category in drug development (SI>1), making it a potential candidate for treating inflammation (22).

Conclusion

The present study demonstrated the antioxidant and anti-inflammatory potential of *C. papaya* L. leaf alkaloid fraction in *in vitro* conditions. UPLC-Q-TOF-MS/

MS analysis identified that carpaine and carpamic acid could be the potential alkaloid compounds. The alkaloid fraction demonstrated significant antioxidant and anti-inflammatory potential, indicating its therapeutic relevance in managing disease conditions such as thrombocytopenia. *In silico* analysis revealed that hydrogen bonding was the predominant mode of interaction between the alkaloid compounds and the pro-inflammatory enzymes COX-2 and iNOS. Carpamic acid demonstrated a stronger binding affinity towards both enzymes than carpaine. The selectivity index of the fraction falls under the favorable category of drug development. Further investigation in *in vivo* models is recommended to validate its application as a therapeutic agent.

Acknowledgments

The first author is an awardee of the Senior Research Fellowship (SRF), University Grants Commission (UGC). The authors are grateful to Mr. Cyrus Mathew Koshy of the Inter-University Instrumentation Centre (IUIC), Mahatma Gandhi University, Kottayam, Kerala, for providing technical support for UPLC-Q-ToF-MS/MS analysis. We acknowledge Dr. Dileep K. Vijayan, Visiting Scientist at the Laboratory for Structural Bioinformatics, RIKEN, for his valuable discussions and for providing access to computational resources.

Authors' contribution

Conceptualization: Arya J, Mathew John, Krishnakumar K.
Data curation: Arya J, Krishnakumar K, Mathew John, Alex George.
Formal analysis: Arya J, Alex George.
Funding acquisition: Arya J, Mathew John.
Investigation: Arya J, Mathew John.
Methodology: Arya J, Mathew John, Krishnakumar K, Remya Chandran, Akash Prakash.
Project administration: Mathew John.
Resources: Arya J, Mathew John, Akash Prakash.
Software: Alex George, Remya Chandran.
Supervision: Krishnakumar K, Mathew John.
Validation: Mathew John, Krishnakumar K.
Visualization: Arya J, Akash Prakash.
Writing–original draft: Arya J.
Writing–review & editing: Arya J, Mathew John, Krishnakumar K, Alex George, Remya Chandran, Akash Prakash.

Conflict of interests

The authors declared no conflict of interest

Ethical considerations

All ethical concerns, including plagiarism, falsification, data fabrication, and copyright infringement, were fully addressed. The present study did not involve the use of human or animal subjects.

Funding/Support

The current study has not received any external grants from funding agencies, including those from public, commercial, or not-for-profit sectors. The first author is an awardee of a Senior Research Fellowship from the UGC.

References

1. Koul B, Pudhuvai B, Sharma C, Kumar A, Sharma V, Yadav D, et al. *Carica papaya* L.: a tropical fruit with benefits beyond the tropics. Diversity. 2022;14(8):683. doi: 10.3390/d14080683.
2. Ugbogu EA, Dike ED, Uche ME, Etumnu LR, Okoro BC, Ugbogu OC, et al. Ethnomedicinal uses, nutritional composition, phytochemistry and potential health benefits of *Carica papaya*. Pharmacol Re Mod Chin Med. 2023;7:100266. doi: 10.1016/j.prmcm.2023.100266.
3. Dharmarathna SL, Wickramasinghe S, Waduge RN, Rajapakse RP, Kularatne SA. Does *Carica papaya* leaf-extract increase the platelet count? An experimental study in a murine model. Asian Pac J Trop Biomed. 2013;3(9):720-4. doi: 10.1016/s2221-1691(13)60145-8.
4. Sathyapalan DT, Padmanabhan A, Moni M, B PP, Prasanna P, Balachandran S, et al. Efficacy & safety of *Carica papaya* leaf extract (CPLE) in severe thrombocytopenia (≤30,000/µl) in adult dengue - results of a pilot study. PLoS One. 2020;15(2):e0228699. doi: 10.1371/journal.pone.0228699.
5. Anjum V, Arora P, Ansari SH, Najmi AK, Ahmad S. Antithrombocytopenic and immunomodulatory potential of metabolically characterized aqueous extract of *Carica papaya* leaves. Pharm Biol. 2017;55(1):2043-56. doi: 10.1080/13880209.2017.1346690.
6. Burdick EM. Carpaine: an alkaloid of *Carica papaya*—its chemistry and pharmacology. Econ Bot. 1971;25(4):363-5. doi: 10.1007/bf02985202.
7. Julianti T, De Mieri M, Zimmermann S, Ebrahimi SN, Kaiser M, Neuburger M, et al. HPLC-based activity profiling for antiplasmodial compounds in the traditional Indonesian medicinal plant *Carica papaya* L. J Ethnopharmacol. 2014;155(1):426-34. doi: 10.1016/j.jep.2014.05.050.
8. Sudi S, Chin YZ, Wasli NS, Fong SY, Shimmi SC, How SE, et al. Carpaine promotes proliferation and repair of H9c2 cardiomyocytes after oxidative insults. Pharmaceuticals (Basel). 2022;15(2):230. doi: 10.3390/ph15020230.
9. Zunjar V, Dash RP, Jivrajani M, Trivedi B, Nivsarkar M. Antithrombocytopenic activity of carpaine and alkaloidal extract of *Carica papaya* Linn. leaves in busulfan induced thrombocytopenic Wistar rats. J Ethnopharmacol. 2016;181:20-5. doi: 10.1016/j.jep.2016.01.035.
10. Goerge T, Ho-Tin-Noe B, Carbo C, Benarafa C, Remold-O'Donnell E, Zhao BQ, et al. Inflammation induces hemorrhage in thrombocytopenia. Blood. 2008;111(10):4958-64. doi: 10.1182/blood-2007-11-123620.
11. Das S, Abreu C, Harris M, Shrader J, Sarvepalli S. Severe thrombocytopenia associated with dengue fever: an evidence-based approach to management of thrombocytopenia. Case Rep Hematol. 2022;2022:3358325.

doi: 10.1155/2022/3358325.
12. Kuczera D, Assolini JP, Tomiotto-Pellissier F, Pavanelli WR, Silveira GF. Highlights for dengue immunopathogenesis: antibody-dependent enhancement, cytokine storm, and beyond. J Interferon Cytokine Res. 2018;38(2):69-80. doi: 10.1089/jir.2017.0037.
13. Nakao S, Lai CJ, Young NS. Dengue virus, a flavivirus, propagates in human bone marrow progenitors and hematopoietic cell lines. Blood. 1989;74(4):1235-40.
14. Hottz E, Tolley ND, Zimmerman GA, Weyrich AS, Bozza FA. Platelets in dengue infection. Drug Discov Today Dis Mech. 2011;8(1-2):e33-8. doi: 10.1016/j.ddmec.2011.09.001.
15. Wang X, Hu C, Ai Q, Chen Y, Wang Z, Ou S. Isolation and identification carpaine in *Carica papaya* L. leaf by HPLC-UV method. Int J Food Prop. 2015;18(7):1505-12. doi: 10.1080/10942912.2014.900785.
16. Kumar SS, Krishnakumar K, John M. Flavonoids from the butanol extract of *Carica papaya* L. cultivar 'Red Lady' leaf using UPLC-ESI-Q-ToF-MS/MS analysis and evaluation of the antioxidant activities of its fractions. Food Chem Adv. 2022;1:100126. doi: 10.1016/j.focha.2022.100126.
17. Rusli R, Ramadhan DS, Rusdiaman R, Fakih TM. Evaluating quercetin analogs from Indonesian bioflavonoids for breast cancer: insights from in silico and cytotoxicity assays. J Herbmed Pharmacol. 2025;14(4):417-25. doi: 10.34172/jhp.2025.52829.
18. Thangadurai TD, Manjubaashini N, Sowndarya A, Subitha A, Kausalya G, Shanmugaraju S, et al. Multipurpose biological applications of excitation-dependent fluorescent carbon nano dots emanated from biomass waste. Mater Chem Phys. 2023;307:128113. doi: 10.1016/j.matchemphys.2023.128113.
19. Walker MC, Gierse JK. In vitro assays for cyclooxygenase activity and inhibitor characterization. Methods Mol Biol. 2010;644:131-44. doi: 10.1007/978-1-59745-364-6_11.
20. Salter M, Duffy C, Garthwaite J, Strijbos PJ. Ex vivo measurement of brain tissue nitrite and nitrate accurately reflects nitric oxide synthase activity in vivo. J Neurochem. 1996;66(4):1683-90. doi: 10.1046/j.1471-4159.1996.66041683.x.
21. Lepoivre M, Chenais B, Yapo A, Lemaire G, Thelander L, Tenu JP. Alterations of ribonucleotide reductase activity following induction of the nitrite-generating pathway in adenocarcinoma cells. J Biol Chem. 1990;265(24):14143-9.
22. Adebayo SA, Steel HC, Shai LJ, Eloff JN. Investigation of the mechanism of anti-inflammatory action and cytotoxicity of a semipurified fraction and isolated compounds from the leaf of *Peltophorum africanum* (Fabaceae). J Evid Based Complementary Altern Med. 2017;22(4):840-5. doi: 10.1177/2156587217717417.
23. Kumar SS, Remya C, Krishnakumar K, Maria E, Dileep KV, John M. Modulation of COX-2, 5-LOX, and cytokine signalling by *Carica papaya* L. leaf cultivar 'Red Lady' flavonoids in inflammation: in-vitro and in-silico insights. Nat Prod Res. 2025:1-7. doi: 10.1080/14786419.2025.2566471.
24. Li H, Jamal J, Delker S, Plaza C, Ji H, Jing Q, et al. The mobility of a conserved tyrosine residue controls isoform-dependent enzyme-inhibitor interactions in nitric oxide synthases. Biochemistry. 2014;53(32):5272-9. doi: 10.1021/bi500561h.
25. Marin-Palma D, Sirois CM, Urcuqui-Inchima S, Hernandez JC. Inflammatory status and severity of disease in dengue patients are associated with lipoprotein alterations. PLoS One. 2019;14(3):e0214245. doi: 10.1371/journal.pone.0214245.
26. Zevini A, Ferrari M, Olagnier D, Hiscott J. Dengue virus infection and Nrf2 regulation of oxidative stress. Curr Opin Virol. 2020;43:35-40. doi: 10.1016/j.coviro.2020.07.015.
27. Soundravally R, Hoti SL, Patil SA, Cleetus CC, Zachariah B, Kadhiravan T, et al. Association between proinflammatory cytokines and lipid peroxidation in patients with severe dengue disease around defervescence. Int J Infect Dis. 2014;18:68-72. doi: 10.1016/j.ijid.2013.09.022.
28. Charlton NC, Mastyugin M, Török B, Török M. Structural features of small molecule antioxidants and strategic modifications to improve potential bioactivity. Molecules. 2023;28(3):1057. doi: 10.3390/molecules28031057.
29. Krishnakumar K, Augusti KT, Vijayammal PL. Anti-peroxidative and hypoglycaemic activity of *Salacia oblonga* extract in diabetic rats. Pharm Biol. 2000;38(2):101-5. doi: 10.1076/1388-0209(200004)3821-1ft101.
30. Asghar N, Naqvi SA, Hussain Z, Rasool N, Khan ZA, Shahzad SA, et al. Compositional difference in antioxidant and antibacterial activity of all parts of the *Carica papaya* using different solvents. Chem Cent J. 2016;10:5. doi: 10.1186/s13065-016-0149-0.
31. Khor BK, Chear NJ, Azizi J, Khaw KY. Chemical composition, antioxidant and cytoprotective potentials of *Carica papaya* leaf extracts: a comparison of supercritical fluid and conventional extraction methods. Molecules. 2021;26(5):1489. doi: 10.3390/molecules26051489.
32. Helen A, Krishnakumar K, Vijayammal PL, Augusti KT. A comparative study of antioxidants S-allyl cysteine sulfoxide and vitamin E on the damages induced by nicotine in rats. Pharmacology. 2003;67(3):113-7. doi: 10.1159/000067796.
33. Agada R, Usman WA, Shehu S, Thagariki D. In vitro and in vivo inhibitory effects of *Carica papaya* seed on α-amylase and α-glucosidase enzymes. Heliyon. 2020;6(3):e03618. doi: 10.1016/j.heliyon.2020.e03618.
34. Tan WS, Arulselvan P, Karthivashan G, Fakurazi S. *Moringa oleifera* flower extract suppresses the activation of inflammatory mediators in lipopolysaccharide-stimulated RAW 264.7 macrophages via NF-κB pathway. Mediators Inflamm. 2015;2015:720171. doi: 10.1155/2015/720171.
35. Neves-Souza PC, Azeredo EL, Zagne SM, Valls-de-Souza R, Reis SR, Cerqueira DI, et al. Inducible nitric oxide synthase (iNOS) expression in monocytes during acute dengue fever in patients and during in vitro infection. BMC Infect Dis. 2005;5:64. doi: 10.1186/1471-2334-5-64.
36. Cheng YL, Lin YS, Chen CL, Wan SW, Ou YD, Yu CY, et al. Dengue virus infection causes the activation of distinct NF-κB pathways for inducible nitric oxide synthase and TNF-α expression in RAW264.7 cells. Mediators Inflamm. 2015;2015:274025. doi: 10.1155/2015/274025.
37. Rouzer CA, Marnett LJ. Cyclooxygenases: structural and functional insights. J Lipid Res. 2009;50 Suppl:S29-34. doi: 10.1194/jlr.R800042-JLR200.

Copyright © 2026 The Author(s). This is an open-access article distributed under the terms of the Creative Commons Attribution License (http://creativecommons.org/licenses/by/4.0), which permits unrestricted use, distribution, and reproduction in any medium, provided the original work is properly cited.